

Video Article

Study of the Actin Cytoskeleton in Live Endothelial Cells Expressing GFP-Actin

Travis M. Doggett¹, Jerome W. Breslin¹

¹Department of Physiology, Louisiana State University Health Sciences Center

Correspondence to: Jerome W. Breslin at jbresl@lsuhsc.edu

URL: <https://www.jove.com/video/3187>

DOI: [doi:10.3791/3187](https://doi.org/10.3791/3187)

Keywords: Cell Biology, Issue 57, Endothelial cells, actin, cytoskeleton, live-cell imaging, GFP, lamellipodia, stress fibers, kymograph analysis

Date Published: 11/18/2011

Citation: Doggett, T.M., Breslin, J.W. Study of the Actin Cytoskeleton in Live Endothelial Cells Expressing GFP-Actin. *J. Vis. Exp.* (57), e3187, doi:10.3791/3187 (2011).

Abstract

The microvascular endothelium plays an important role as a selectively permeable barrier to fluids and solutes. The adhesive junctions between endothelial cells regulate permeability of the endothelium, and many studies have indicated the important contribution of the actin cytoskeleton to determining junctional integrity¹⁻⁵. A cortical actin belt is thought to be important for the maintenance of stable junctions^{1,2,4,5}. In contrast, actin stress fibers are thought to generate centripetal tension within endothelial cells that weakens junctions²⁻⁵. Much of this theory has been based on studies in which endothelial cells are treated with inflammatory mediators known to increase endothelial permeability, and then fixing the cells and labeling F-actin for microscopic observation. However, these studies provide a very limited understanding of the role of the actin cytoskeleton because images of fixed cells provide only snapshots in time with no information about the dynamics of actin structures⁵.

Live-cell imaging allows incorporation of the dynamic nature of the actin cytoskeleton into the studies of the mechanisms determining endothelial barrier integrity. A major advantage of this method is that the impact of various inflammatory stimuli on actin structures in endothelial cells can be assessed in the same set of living cells before and after treatment, removing potential bias that may occur when observing fixed specimens. Human umbilical vein endothelial cells (HUVEC) are transfected with a GFP- β -actin plasmid and grown to confluence on glass coverslips. Time-lapse images of GFP-actin in confluent HUVEC are captured before and after the addition of inflammatory mediators that elicit time-dependent changes in endothelial barrier integrity. These studies enable visual observation of the fluid sequence of changes in the actin cytoskeleton that contribute to endothelial barrier disruption and restoration.

Our results consistently show local, actin-rich lamellipodia formation and turnover in endothelial cells. The formation and movement of actin stress fibers can also be observed. An analysis of the frequency of formation and turnover of the local lamellipodia, before and after treatment with inflammatory stimuli can be documented by kymograph analyses. These studies provide important information on the dynamic nature of the actin cytoskeleton in endothelial cells that can be used to discover previously unidentified molecular mechanisms important for the maintenance of endothelial barrier integrity.

Video Link

The video component of this article can be found at <https://www.jove.com/video/3187/>

Protocol

1. Transfection of HUVEC with GFP-actin

1. Various methods can be used to transfect HUVEC. Our lab uses the Nucleofector system (Lonza, Basel Switzerland) outlined below. In general, work quickly to improve cell viability and transfection efficiency. Each transfection requires 5×10^5 HUVEC that will be seeded onto two glass coverslips (Corning No. 1, 22 x 50 mm). The Nucleofector combines electroporation and chemical reagents to transfect plasmid DNA, and typically achieves an >50% expression efficiency. Chemical transfection reagents are an alternative method. One group has successfully transfected bovine endothelial cells with GFP-actin using the GenePORTER reagent⁶. The Nucleofector protocol we use is described below.
2. Presterilized cultureware or ordinary coverslips can be used, depending on the chamber type. For glass coverslips, sterilize in a biological safety hood by placing them into a 10 cm culture plate containing approximately 5 ml of 70% ethanol for 2 min. Pick them up with sterile forceps and air dry by leaning them against the side of a separate culture plate.
3. Once dry, place each coverslip in its own 10 cm culture plate. Pipette a 300 μ L bead of warm gelatin solution (1.5% in 0.9% NaCl) on the center of the coverslip and allow it to stand for 5 min., and then aspirate. Keeping this matrix coating in the center, without touching the edges, will ensure that the cells will be seeded densely and will achieve confluence quickly.
4. Prepare one 1.5 mL microfuge tube per transfection with 500 μ L of EGM2MV media (Lonza) and set aside in a 37°C, 5% CO₂ incubator.

5. Detach HUVEC with 0.25% trypsin-EDTA and collect into a 15 mL conical tube. Count the cells. 5×10^5 cells are needed for each transfection. Adjust the cell suspension volume to obtain a pellet that will contain 5×10^5 cells multiplied by the number of transfections to be performed.
6. Centrifuge the cell suspension in a clinical centrifuge at 5000 rpm for 3 minutes at room temperature. Aspirate the supernatant by tilting the tube to remove as much media as possible.
7. Resuspend the pellet with Basic Nucleofector Solution from either the HUVEC or Primary Endothelial Cell Nucleofector Kit (Lonza). Use 100 μL per 5×10^5 cells. Due to the toxicity of this solution, it is important to work quickly while the cells are suspended in this solution.
8. Add the GFP- β -actin vector plasmid (0.2-2 μg per 100 μL of Nucleofector suspension) to the transfection sample. 0.2-2 μg of GFP-actin plasmid DNA per 5×10^5 cells per transfection.
9. Transfer 100 μL of cell suspension to a Nucleofector Cuvette. Cover and tap the cuvette a few of times to ensure the cell suspension is all the way to the bottom.
10. Place the cuvette into the Nucleofector II device cuvette slot and run the desired electroporation program. We use program A-034 for HUVEC.
11. Return the cuvette to the biological safety hood. Bring one of the microfuge tubes from the 37 °C incubator that contains 500 μL of EGM2MV to the hood. Using one of the transfer pipettes provided in the Nucleofector kit, gently add the warm 500 μL of media to the cell suspension in the cuvette. Transfer all of the contents of the cuvette back to the microfuge tube and place in the incubator for 15 min. to allow the cells to recover.
12. Repeat steps 9-11 as needed if more cells are to be transfected.
13. One microfuge tube containing 600 μL of transfected HUVEC suspension can be seeded onto two coverslips. Under the hood and with a 1000 μL micropipette, gently pipette up and down once to mix the suspension, and then place 300 μL of the suspension directly onto a gelatin-coated coverslip. Do not let the suspension touch the edge of the coverslip. Place in the 37 °C/5% CO_2 incubator for 1-4 h to allow for cell attachment.
14. After 1-4 h, inspect the transfected cells to confirm they have attached to the coverslip. Then add 10 mL of EGM2MV media, and return to the plate to the 37°C/5% CO_2 incubator. GFP-actin expression can typically be observed within 4-8 hours. Experiments are typically performed within 24-48 h.

2. Setting up the live-cell imaging chamber and stage heater

1. For most of our studies, we have used a Warner Instruments open diamond bath (RC22) placed in a PH-1 stage heater, fed by a gravity flow system. However, several options are available for live cell imaging stages, including chambers that accommodate glass bottom culture dishes, open vs. closed chambers, and various microincubator/objective heater combinations and large incubator systems. Ultimately, the chamber selection will depend upon factors including the need to access the bath to add a test agent or drug, whether the medium will be static or under flow, and the length of the experiment. In addition, sometimes factors like temperature instability can cause focus drift, and can be minimized by control systems that can maintain stable bath and objective temperatures.
2. Aliquot enough medium for the experiment. We aliquot 50 ml of albumin physiological salt solution (APSS; Table 1) for each hour the experiment will last.
3. Either a pump or gravity-flow system can be used to deliver medium to the chamber. For our system, we add APSS to a simple gravity-flow system built from an intravenous flow line, connected to an inline heater (Warner Instruments model SH-27A). We apply flow at approximately 40 mL/h.
4. If an open bath chamber like ours will be used, apply vacuum grease to the outer edge on the underside of the diamond bath and with a cotton-tipped applicator. Next, we get one cell-covered coverslip from the incubator, and gently lift the coverslip using forceps. Gently touch the backside to a kimwipe to soak up excess medium while keeping the cell-covered side wet. With the cells face up, place the diamond bath over the coverslip to form a chamber.
5. Quickly place the chamber into the stage heater and hand-tighten the clamps over the chamber. A major concern at this stage is the possibility that the cells will dry out. Therefore it is important to work quickly and when done, immediately pipette -1 mL of medium into the chamber to prevent the cells from drying out.
6. Our chamber allows for steady flow of the medium over the cells. Just before turning on flow, it is important to attach a vacuum hose to its holder on the chamber to permit exit of excess culture medium (APSS). The inline heater and bath heater should also be turned on at this point (to 37 °C). Our system also has a thermistor probe to monitor temperature, which should be placed on the edge of the bath.
7. Carefully wipe the underside of the coverslip with a kimwipe soaked with 70% EtOH to remove remaining EGM2MV media and salt buildup. Wipe a second time with a dry kimwipe or lens paper.
8. After the chamber has been set up, flow is on, and the temperature is steady at 37 °C, allow the cells at least 30 minutes to adjust and stabilize before starting the experiment.
9. While waiting, turn on all the components of the live-cell imaging microscope (lamps, filter wheel controller, camera, computer).

3. Acquisition of data with live-cell imaging microscope

1.
 - Various live cell microscopy systems are available. Our system is a Nikon Eclipse TE-2000U with the following components:
 - Sutter Instruments Lambda LS 300 W xenon lamp
 - Sutter Instruments Lambda 10-3 excitation filter wheel with SmartShutter and S492 filter (D350 and S572 exciter filters are also available for UV and RFP applications)
 - Dichroic 2002bs emitter (Nikon 61002m)
 - CI Plan Fluor 10X DLL Objective, NA 0.30 (Nikon MRH10100)
 - Plan Fluor ELWD 40X DM Objective, NA 0.60 (Nikon MRH08420)
 - Plan Apo VC 100X Oil Objective, NA 1.40 (Nikon MRD01901)
 - Photometrics CoolSNAP HQ2 camera, 1392 x 1040 imaging array, 6.45 x 6.45 μm pixels (Roper Scientific)
 - We also have two software packages that can be used for image acquisition. Nikon Elements-AR 3.0, and Metamorph 6.1.

2. After viewing the cells and finding an appropriate area for study, lock the coarse focus knob and check the software acquisition settings so that:
 1. The filter wheel is set for the S492 filter (labeled "FITC" in our configuration)
 2. In the acquisition software, the objective is set to match the desired magnification (our microscope is not motorized, but this sets the $\mu\text{m}/\text{pixel}$ ratio). Also make sure that the optivar lens on the microscope is set to 1.0X magnification. Setting the optivar to 1.5X may increase magnification, however at the expense of losing signal intensity. The magnification to be used depends aims of the study. For the best detail, a 100X objective with a high numerical aperture will provide the best spatial resolution and transmission of signal. Our microscope is also equipped with a long working distance 40X objective intended for a different application that requires the extra distance. However, this objective can be useful when we wish to observe several cells simultaneously, and works fine for viewing organelle-sized structures, however at a cost of losing spatial resolution and signal intensity. For any study in which signal intensity is an endpoint, or for more advanced imaging techniques such as fluorescence speckle microscopy, a 100X objective is recommended.
 3. The camera exposure time is set between 0.5-2 s. This depends on the GFP-actin intensity in the cells. We generally use the lowest possible exposure time to avoid bleaching of the GFP-actin and potential toxicity to the cells.
 4. To achieve the best resolution, the Binning should be set at 1 x 1 and Gain at 1. In some cases we have set binning to 2 x 2 to reduce exposure time, however this reduces the precision of the measurements we can make on moving objects in the time-lapse study.
 5. Configure the time-lapse settings:
 1. Choose the folder to save the captured images and type a filename.
 2. Set the number of images and interval duration times for the experiment. We typically use a 15 s to 1 min interval between images and up to 2 h for the duration.
 3. Make sure that the active shutter is set to be closed between acquisitions.
3. Before starting time-lapse image acquisition, turn off the room lights and capture a single image to check the settings.
4. Also capture a brightfield image. Make sure the condenser is set to the proper phase or DIC filter. Turn on the halogen lamp and collect the image. Turn off the halogen lamp.
5. Revert back to "FITC" settings for the time-lapse imaging and capture a test image.
6. Capture the time-lapse series.

During the experiment, it is important to monitor the images as they are acquired. In some instances small changes in temperature within the chamber may cause focus drift. This can be avoided by optimizing the inflow and vacuum lines so that flow is steady over the cells. Also, minimizing traffic in microscope room, and redirecting drafts from ceiling air vents away from the microscope can be helpful. An alternative that has worked well in our experience is the use of 37 °C/5% CO₂ incubator chambers that enclose the entire stage and objective. These offer the advantage of monitoring cells overnight or longer, but access to the cells is limited. If necessary, pause the time-lapse acquisition and refocus the image. Perform the refocus as quickly as possible to avoid altering the time interval between images.
7. A typical protocol will consist of 20-30 minutes of baseline images before adding a test agent followed by 0.5 to 4 hours of additional image acquisition. The length of the experiment can be limited by photobleaching of the GFP over time, which is why it is important to choose the shortest exposure time possible. It may also be desirable to change the interval between time lapse images to 30-60 s if a longer study is desired.

4. Data analysis

1. Several software packages can be used to analyze the image sets, such as NIS Elements, Metamorph, Slidebook, etc. We typically perform our image analysis using NIH ImageJ enabling analysis on any computer on our lab or at home. The versions we use are: MBF ImageJ (<http://www.macbiophotonics.ca/imagej/>) FIJI (<http://pacific.mpi-cbg.de/wiki/index.php/Fiji>).
2. ImageJ can be used to analyze many dynamic processes, including:
 - *Frequency of lamellipodia protrusions*
 - *Distance, time, and velocity of protrusions*
 - *Actin fiber movement over time*

Nikon Elements saves time-lapse images as an "ND" file. To open in ImageJ this needs to be converted to a TIF series using the "export ND document" feature. Metamorph image stacks can be opened in ImageJ without modification. One option we choose when opening a TIF series in ImageJ is to convert to 8-bit grayscale. This makes viewing easier because adjustments to the brightness and contrast will apply to the entire series rather than the single image being viewed.

3. In ImageJ, when the image set opens the slice number/total slices will be displayed in the top left corner of the window, along with the filename, the number of pixels, file type, and size. The Z scrollbar on the bottom corresponds to time. In addition, hovering the pointer over the image will display the x, y, and z pixel location on the bottom of the ImageJ toolbar.
4. Lamellipodia protrusion can be studied by determining the number of new protrusions over time. This can be done for the entire cell perimeter or a selected region. This type of analysis can also be performed in nonconfluent, untransfected cells with phase contrast or DIC microscopy. However, using cells expressing GFP-actin allows analysis of confluent monolayers, particularly when cells containing and lacking GFP-actin are adjacent to one another.
5. Lamellipodia protrusion distance, persistence (time), and velocity can be assessed by kymograph (line scan) analysis. Draw a line perpendicular to the edge of a cell (this is easiest if there is no adjacent cell, or the adjacent cell does not express GFP-actin). In ImageJ, pressing "/" will generate a kymograph, with the x-axis representing distance and the y-axis representing time (15 s to 1 min per pixel according to the time interval guidelines above). Lines can be drawn over a protruding lamellipodia and the box dimensions measured (by pressing M in ImageJ). The distance, time, and velocity can then be calculated.
6. The movement of stress fibers can also be measured by kymograph analysis in a similar fashion.

5. Representative Results:

With our transfection protocol, we typically see expression of GFP-actin in at least 50% of the HUVEC transfected, and often can find areas on the coverslip where >90% of the HUVEC in the region express GFP-actin. An example of a live cell imaging experiment with subconfluent HUVEC expressing GFP-actin is shown in Movie 1. For this particular experiment, an image was acquired once per minute. As can be seen in the movie, GFP-actin in the HUVEC can be observed throughout the cytoplasm, as well as in filamentous structures and in local lamellipodia protruding along the cell edge. Also apparent in the movie is that GFP-actin expression is not uniform between cells. Cells chosen for study typically have enough GFP-actin present to visualize various structures containing filamentous actin. Cells expressing very high levels of GFP-actin can be problematic for study because in these cells it is typically difficult to distinguish F-actin structures from the high amount of G-actin present.

Movie 2 shows an example of the behavior of confluent HUVEC expressing GFP-actin. Like the subconfluent HUVEC, active lamellipodia formation and turnover along the perimeters of cells was apparent. However, these lamellipodia often gave rise to membrane ruffles, indicating less efficient protrusion⁷. This is probably due to the presence of adjacent cells blocking the nearby substratum. Actin cortical fibers and stress fibers are also visible in Movies 1 and 2. Although the cells we observed remained stationary, the stress fibers are similar to transverse arc fibers in migrating cells, forming near the cell edge and moving laterally toward the cell center where they disassemble^{8,9}. An additional dynamic feature observed in these cells was the formation of actin ring structures that expanded concentrically, previously named actin clouds¹⁰.

An example of how the distance, persistence, and velocity of cell protrusions are quantified from these time-lapse image sets using kymograph analysis is shown in Figure 1. In Figure 1A, a single pixel line is drawn roughly perpendicular to the cell edge for generation of a kymograph (Figure 1B). In this kymograph, the region defined by the line is placed vertically and the images from throughout the time-lapse are stacked horizontally. Looking from left to right in the kymograph, protrusions are represented as upward movements in the edge of the cell. In Figure 1C, a line was superimposed on the edge of one of these protrusions, and the pixel data associated with that line were collected and are shown in the Results window at the bottom of the panel. This analysis allows quantification of protrusion dynamics, and can also be used to estimate the protrusion frequency (number of protrusions/time) in this region of the cell.

An example of the analysis of stress fiber movement is shown in Figure 2. Most stress fibers we observed formed near the cell periphery and moved toward the cell center, where they eventually disassembled. This can also be quantified by kymograph analysis. A line is drawn perpendicular to the cell edge and to the stress fibers (Figure 2A) and a kymograph is generated (Figure 2B). The stress fibers appear as continuous lines in the cytoplasmic area in the kymograph, often moving down and to the right (toward the cell center). Sometimes the fibers are difficult to see in the original kymograph, and in these cases we use the unsharp mask filter to sharpen the image (Figure 2C). Lines are drawn on the stress fibers and the pixel data are collected using the measure function (Figure 2D). An alternative way to collect this data is to draw a line from the start to finish of the identified stress fiber to get the average slope for the duration that the fiber was observed (Figure 2E). This analysis allows quantification of stress fiber lateral movement and can also be used to quantify the number of stress fibers observed in this region of the cell.

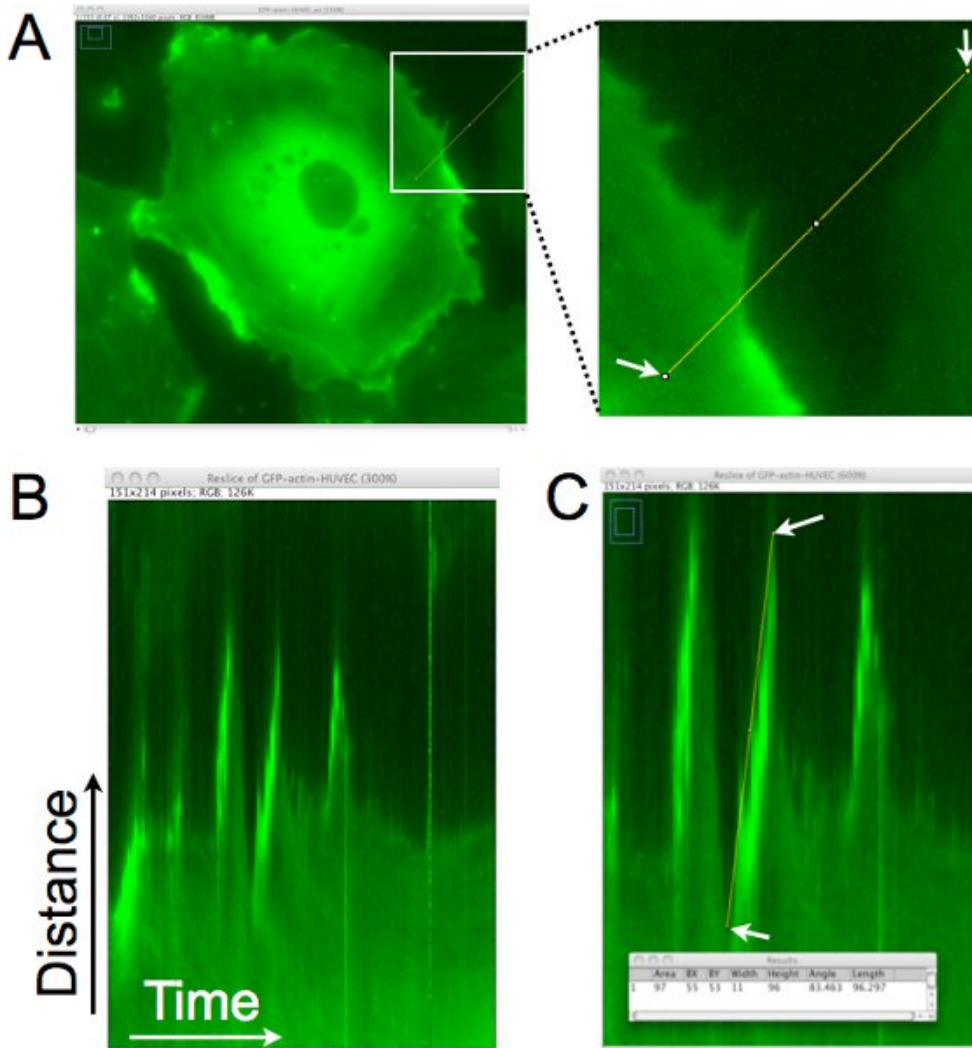


Figure 1. Kymograph analysis of the cell edge to determine the protrusion distance, persistence, and velocity of local lamellipodia. **A.** A single pixel line is drawn roughly perpendicular to the edge of the cell. This region is extracted from each image of the time-lapse set to generate a montage of the region over time. **B.** In the resulting kymograph, the x-axis represents time, moving from left to right, and the y-axis shows distance. Movement of the cell edge over time can be evaluated in this kymograph, and lamellipodia are identified regions where the cell edge, moving rightward, goes upward. **C.** A line is drawn on the cell edge where a protrusion by a lamellipodium has been identified. The dimensions of the bounding rectangle for the line drawn are then acquired (shown in superimposed window). The width is used to calculate the protrusion time or persistence. The height is used to calculate the protrusion distance. The protrusion velocity is calculated by dividing the height by the width. In this example, the upward distance was 96 pixels x 0.16125 $\mu\text{m}/\text{pixel}$ = 15.5 μm , and the time was 11 pixels x 1 min./pixel = 11 min. The velocity was calculated as 15.5 $\mu\text{m}/11$ min. = 1.4 $\mu\text{m}/\text{min}$.

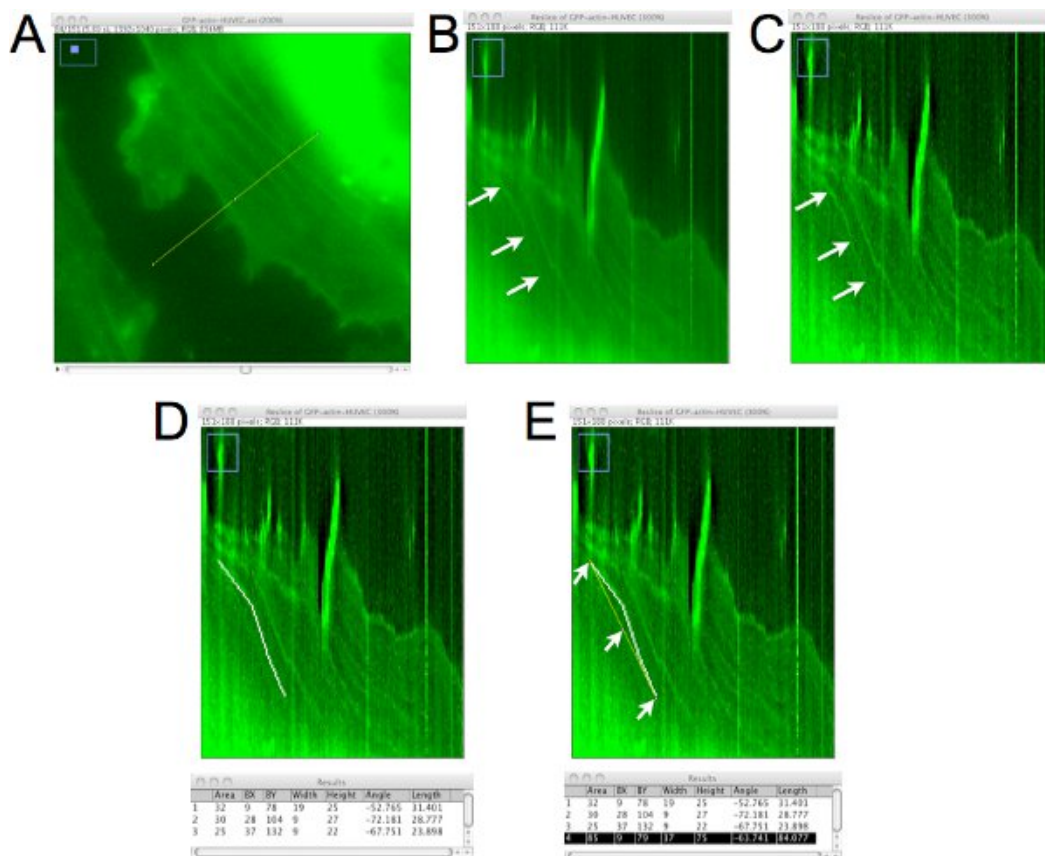


Figure 2. Kymograph analysis of the movement of actin stress fibers. *A.* A single pixel line is drawn perpendicular to the edge of the cell to generate a kymograph. *B.* As shown in Fig. 1, in the resulting kymograph, the x-axis represents time and the y-axis distance. Stress fibers are observed as continuous lines in the cell, often going downward and to the right (arrows) *C.* To better visualize the stress fibers, the unsharp mask filter can be used. In this example, a radius of 3 pixels and mask weight of 0.60 was used. *D.* Single pixel lines are then drawn over the identified stress fiber, and data collected. In this panel three lines were drawn and then "delete" was pressed to make a permanent annotation (white line) of their locations after each measurement. *E.* Alternatively, if the average distance, time, and velocity of the stress fiber is desired, a line can be drawn from the start and finish points (yellow line), and the data for that can be acquired (highlighted in the Results window). For this example, the measurements were made on this stress fiber for 37 frames x 1 frame/min. = 37 min. The distance traveled over this time period was 75 frames x 0.16125 $\mu\text{m}/\text{pixel}$ = 12.1 μm . The resulting lateral velocity of the stress fiber was 12.1 $\mu\text{m}/37\text{min}$ = +0.33 $\mu\text{m}/\text{min}$. A positive value for velocity is assigned for fibers moving toward the cell center, and negative for fibers moving toward the periphery.

Movie 1. Time-lapse images of live HUVEC expressing GFP-actin. The interval between images is 1 min. Local lamellipodia protruded along the entire perimeter of cells. In addition, transverse arc stress fibers moved laterally toward the center of cells. When thrombin (1 U/ml) was added to the bath, the cells contracted slightly and the outward protrusions of lamellipodia paused for about 10 min. After the cells contracted, lamellipodia formation and turnover resumed. [Click here to watch the movie.](#)

Movie 2. Confluent HUVEC expressing GFP-actin, before and after treatment with thrombin. Elapsed time is shown in the bottom right corner as minutes:seconds. The interval between images is 30 s. Thrombin (1 U/ml) was added after the 45 min. baseline period. Annotated events include local lamellipodia formation and turnover (arrowheads near cell edges, 0:59 - 37:29), actin clouds (arrows, 1:59 - 21:29), and a gap at a tricellular junction that widens after thrombin is added (arrow, 62:30 - 70:00). Transverse arc stress fibers are also apparent in several of the cells. The cells displayed active formation and turnover of local lamellipodia along their perimeters, with many giving rise to membrane ruffles. Thrombin caused a pause in lamellipodia formation and turnover, and the brief appearance of some small gaps between cells. [Click here to watch the movie.](#)

Discussion

The imaging of GFP-actin in live endothelial cells enables a detailed analysis of the dynamics of the actin cytoskeleton in response to inflammatory stimuli. This method may also be useful to build upon previous findings showing remodeling of the cytoskeleton in response to physical forces like shear stress¹¹. In addition, this method allows a detailed assessment of the contribution of actin cytoskeletal dynamics to various endothelial cell activities, including migration, mitosis, formation of intercellular junctions and junctional maturation, and maintenance of barrier function.

In the data shown, the behavior of the endothelial actin cytoskeleton can be observed before and after treatment with thrombin. Local lamellipodia all along the edges of endothelial cells were observed forming and regressing over time in both nonconfluent and confluent cell monolayers. Treatment with thrombin briefly interrupted lamellipodia formation and turnover. Thrombin also caused the cells to contract slightly, in agreement with previous reports that thrombin causes actin stress fiber formation and increased centripetal tension development in endothelial

cells¹²⁻¹⁴. However, from live cell imaging studies such as this, the origin of the stress fibers can now be determined. In HUVEC, most of the stress fibers originate at the cell periphery and resemble transverse arc fibers in migrating cells^{8,9}. Another strength of this method over using fixed cells is that the number of stress fibers can be quantified in individual cells before and after thrombin treatment, eliminating selection bias between experimental groups.

With this protocol we evaluate dynamic motion of the cell edge and actin stress fibers. To understand actin monomer dynamics in endothelial cells, more advanced techniques such as fluorescence recovery after photobleaching (FRAP) or fluorescence speckle microscopy (FSM) can be applied^{15,16}. In addition, because microvascular endothelial cells may represent a better model of microvascular barrier function, optimization of transfection protocols to effectively express GFP-actin in microvascular endothelial cells represents a logical future direction.

In summary, imaging of live endothelial cells expressing GFP-actin represents a powerful tool to determine how the endothelial cell actin cytoskeleton responds to various types of stimuli. Studies using tightly confluent endothelial monolayers will help determine the roles of dynamic structures such as actin-rich lamellipodia and transverse arc stress fibers in endothelial barrier function. In addition, live cell imaging of endothelial cells expressing GFP-actin or other fusion proteins that allow visualization of other subcellular structures will provide detailed spatiotemporal information needed to understand the signaling and structural mechanisms that determine barrier integrity.

Disclosures

No conflicts of interest declared.

Acknowledgements

The GFP- β -actin plasmid was generously provided by Dr. Wayne Orr, LSUHSC-S Department of Pathology, and was amplified in the laboratory of Dr. Becky Worthylake, LSUHSC-NO Department of Pharmacology. This work was supported by grants from the National Institutes of Health (P20 RR-018766) and the American Heart Association (05835386N).

References

1. Spindler, V., Schlegel, N., & Waschke, J. Role of GTPases in control of microvascular permeability. *Cardiovasc. Res.* **87**, 243-253 (2010).
2. Wojciak-Stothard, B. & Ridley, A.J. Rho GTPases and the regulation of endothelial permeability. *Vascul. Pharmacol.* **39**, 187-199 (2002).
3. Yuan, S.Y. Signal transduction pathways in enhanced microvascular permeability. *Microcirculation.* **7**, 395-403 (2000).
4. Birukov, K.G. Small GTPases in mechanosensitive regulation of endothelial barrier. *Microvasc. Res.* **77**, 46-52 (2009).
5. Duran, W.N., Sanchez, F.A., & Breslin, J.W. Microcirculatory Exchange Function. In, Tuma, R.F., Duran, W.N., & Ley, K., eds. *Handbook of Physiology: Microcirculation.* 2nd ed. Elsevier, San Diego, 81-124 (2008).
6. Hu, Y.L. & Chien, S. Dynamic motion of paxillin on actin filaments in living endothelial cells. *Biochem. Biophys. Res. Commun.* **357**, 871-876 (2007).
7. Borm, B., Requardt, R.P., Herzog, V., & Kirfel, G. Membrane ruffles in cell migration: indicators of inefficient lamellipodia adhesion and compartments of actin filament reorganization. *Exp. Cell. Res.* **302**, 83-95 (2005).
8. Hotulainen, P. & Lappalainen, P. Stress fibers are generated by two distinct actin assembly mechanisms in motile cells. *J. Cell. Biol.* **173**, 383-394 (2006).
9. Pellegrin, S. & Mellor, H. Actin stress fibres. *J. Cell. Sci.* **120**, 3491-3499 (2007).
10. Ballestrem, C., Wehrle-Haller, B., & Imhof, B.A. Actin dynamics in living mammalian cells. *J. Cell. Sci.* **111** (Pt 12), 1649-1658 (1998).
11. Helmke, B.P., Rosen, A.B., & Davies, P.F. Mapping mechanical strain of an endogenous cytoskeletal network in living endothelial cells. *Biophys. J.* **84**, 2691-2699 (2003).
12. Birukova, A.A., Smurova, K., Birukov, K.G., Kaibuchi, K., Garcia, J.G., & Verin, A.D. Role of Rho GTPases in thrombin-induced lung vascular endothelial cells barrier dysfunction. *Microvasc. Res.* **67**, 64-77 (2004).
13. van Nieuw Amerongen, G.P., van Delft, S., Vermeer, M.A., Collard, J.G., & van Hinsbergh, V.W. Activation of RhoA by thrombin in endothelial hyperpermeability: role of Rho kinase and protein tyrosine kinases. *Circ. Res.* **87**, 335-340 (2000).
14. Moy, A.B., Blackwell, K., & Kamath, A. Differential effects of histamine and thrombin on endothelial barrier function through actin-myosin tension. *Am J Physiol Heart Circ Physiol.* **282**, H21-29 (2002).
15. Wittman, T., Littlefield, R., & Waterman-Storer, C. Fluorescent speckle microscopy of cytoskeletal dynamics in living cells. In: Goldman RD, Spector DL, eds. *Live Cell Imaging: A Laboratory Manual.* Cold Spring Harbor Laboratory Press, 184-204 (2005).
16. Rabut, G. & Ellenberg J. Photobleaching techniques to study mobility and molecular dynamics of proteins in live cells: FRAP, iFRAP, and FLIP. In, Goldman, R.D., Spector, D.L., eds. *Live Cell Imaging: A Laboratory Manual.* Cold Spring Harbor Laboratory Press, 101-126 (2005).